ChemComm

Accepted Manuscript

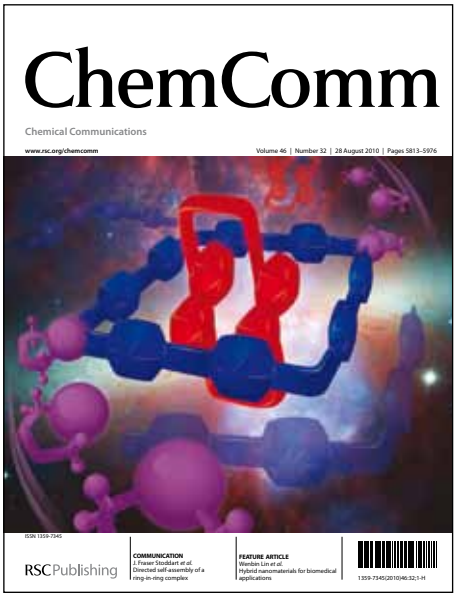

This is an *Accepted Manuscript*, which has been through the RSC Publishing peer review process and has been accepted for publication.

Accepted Manuscripts are published online shortly after acceptance, which is prior to technical editing, formatting and proof reading. This free service from RSC Publishing allows authors to make their results available to the community, in citable form, before publication of the edited article. This *Accepted Manuscript* will be replaced by the edited and formatted *Advance Article* as soon as this is available.

To cite this manuscript please use its permanent Digital Object Identifier (DOI®), which is identical for all formats of publication.

More information about *Accepted Manuscripts* can be found in the **Information for Authors**.

Please note that technical editing may introduce minor changes to the text and/or graphics contained in the manuscript submitted by the author(s) which may alter content, and that the standard **Terms & Conditions** and the **ethical guidelines** that apply to the journal are still applicable. In no event shall the RSC be held responsible for any errors or omissions in these *Accepted Manuscript* manuscripts or any consequences arising from the use of any information contained in them.

Cite this: DOI: 10.1039/c0xx00000x

www.rsc.org/xxxxxx

ARTICLE TYPE

An omega-like DNA nanostructure upon small molecule introduction to stimulate formation of DNAzyme-aptamer conjugate†

Bingqian Liu, Bing Zhang, Guonan Chen, and Dianping Tang*

Received (in XXX, XXX) Xth XXXXXXXXX 20XX, Accepted Xth XXXXXXXXX 20XX

DOI: 10.1039/b000000x

An omega (Ω)-like DNA nanostructure was for the first time utilized for homogenoues electrochemical monitoring of small molecule (ATP used in this case) based on target-induced formation of DNAzyme-aptamer conjugate without the need of sample separation and washing.

Aptamers are single-stranded nucleic acids isolated from random-sequence DNA or RNA libraries by an *in vitro* selection process termed the systematic evolution of ligands by exponential enrichment (SELEX).[1] These small RNA/DNA molecules can form secondary and tertiary structures capable of specifically binding proteins or other cellular targets.[2] Recently, great efforts have been devoted for advanced development of aptamer-based homogeneous assays to make them clinically relevant for the diseases.[3] The methodology relies on devising a detection principle that is modulated and either turned on or turned off as a result of the binding reaction.[4] Unfortunately, most of the current aptamer-based homogeneous assays are based on detection of fluorescence. Moreover, the assays usually require proprietary or specialty fluorescent labels. In contrast, electrochemistry holds great potential as the next-generation detection strategy because of its high sensitivity, simple instrumentation, and excellent compatibility with miniaturization technologies.[5]

For successful development of aptamer-based homogeneous electrochemical assays, one of the important concerns is to design target-dependant aptamer-transduction signal tags. DNAzymes are DNA molecules with catalytic activity.[6] Recent researches demonstrated that some G-quadruplex DNA aptamers have been found to strongly bind hemin to form DNAzymes with peroxidase-like activity.[7] More favourably, hemin-binding G-quadruplex (DNAzyme) exhibits catalytic behaviour towards H_2O_2-mediated oxidation.[8] In this regard, our motivation herein is to design target-triggered transformation of the aptamer-based conformational switch accompanying the formation of DNAzyme.

Recently, omega-like (Ω) DNA nanostructures have attracted great attention in the biomolecular recognition events. Typically, the structure of Ω DNA nanostructures usually consist of two oligonucleotide strands: one strand is complementary to the bases at two ends of another strand. The Willner group designed a series of omega-like DNA nanostructures for the detection of nucleic acids or proteins,[9a] *e.g.*, by using the integration of predesigned DNA constructs that activate logic gate operations,[9b] and aptamer-ATP complex-triggered activation of DNAzyme for release of anticancer drug.[9c] Inspired by the examples, we devise a new omega-like DNA nanostructure (Scheme 1): Strand A (S_A) comprises of anti-target aptamer and hemin-based aptamer with a loop structure in the middle, which can be elaborately blocked by strand B (S_B) with the stems of strand B.

Adenosine triphosphate (ATP) is one of the end products of photophosphorylation, cellular respiration, and fermentation and used by enzymes and structural proteins in many cellular processes.[10] In this work, we report on the proof-of-concept of a powerfully homogeneous electronic monitoring protocol for the detection of ATP by using an omega-like (Ω) DNA nanostructure as the recognition element (Scheme 1, see ESI† for experimental details). Initially, the Ω DNA nanostructures were formed by mixing strand A with strand B with the ratio of 1 : 1. In the presence of target ATP and hemin, target ATP triggered the ATP-based aptamer at 5' end of strand A, resulting in the opening of the Ω DNA nanostructures (*Note*: Hemin alone could not cause the opening of the Ω DNA nanostructures). The released aptamer at 3' end of strand A could intercalate with the hemin, and form the DNAzyme. The formed DNAzyme could catalyze the oxidation of *o*-phenylenediamine (OPD) with the aid of hydrogen peroxide (H_2O_2), resulting in the production of electrochemical signal. By monitoring the change in the signal, we could quantitatively determine the concentration of target ATP in the sample without the need of sample separation and multi-step washing. In the absence of target ATP, the DNAzyme with catalytic activity could almost not be formed, thereby displaying a weak electrochemical signal (background current).

To realize our design, one precondition for the development of homogeneous electrochemical assay was whether the DNAzyme could be formed in the absence and presence of target ATP (*i.e.*, whether the hemin could also induce the opening of Ω DNA nanostructures to form the DNAzyme). To demonstrate this point, the voltammetric characteristics of the as-prepared Ω DNA nanostructures were studied by using square wave voltammetry (SWV) in pH 6.8 Britton-Robinson (BR) buffer containing 0.02 M OPD and 0.02% (v/v) H_2O_2 after incubation with hemin and ATP, respectively (Fig. 1A). As shown from curve '*a*', a low background current was observed at the Ω DNA nanostructures in the buffer. Significantly, the SWV peak current was not almost changed upon addition of 10 μM hemin in the buffer (curve '*b*').

In contrast, the current increased with the simultaneous introduction of 10 μM hemin and 0.1 nM ATP in the buffer (curve '*c*'). Importantly, the electrochemical signal further increased with the increasing target ATP concentration (10 nM) (curve '*d*'). The results indicated that (i) hemin alone could not almost trigger the formation of DNAzyme in the absence of target ATP, and (ii) the detectable signal increased with the increment of target ATP in the sample.

Logically, another question arises as to whether target ATP could really result in the opening of the Ω DNA nanostructures, rather than the hemin. To clarify this issue, we used gel electrophoresis to investigate the Ω DNA nanostructures under the different conditions (Fig. 1B). As shown from lane '*b*', the as-prepared Ω DNA nanostructures had a single strong spot. When the Ω DNA nanostructures were incubated with the high-concentration ATP, however, two spots were acquired (lane '*c*'). These two spots derived from the released strand B (bottom) and the formed ATP-aptamer conjugates with strand A (top), respectively. More interestingly, only one single spot similar to lane '*b*' could be appeared when the hemin was added to the DNA nanostructures (lane '*d*'). The results were almost in accordance with those obtained by the SWV. The slight difference might be attributed to the very weak reaction between hemin and Ω DNA nanostructures. When the Ω DNA nanostructures were incubated with hemin and target ATP, one weak spot (bottom) and one strong spot (top) were achieved (lane '*e*'). The strong spot originated from the formed ATP-aptamer-DNAzyme conjugates. Compared with lane '*c*' (top), the formation of DNAzyme with ATP-aptamer (top spot in lane '*e*') removed slowly in the gel electrophoresis because of the introduction of hemin. Based on these results, we might make preliminarily a conclusion that the designed strategy could be used for the detection of target ATP.

To achieve an optimal electrochemical signal for the developed homogeneous assay protocol, some experimental conditions including pH of the assay solution and incubation time for the formation of DNAzyme conjugates should be investigated. Fig. 2a shows the effect of various pH values of BR buffer on the SWV peak currents of the homogeneous assay system (0.1 nM ATP used as an example). As indicated from Fig. 2a, an optimal current was obtained at pH 6.8 BR buffer. Higher or lower pHs results in the decrease of the electrochemical signals. At the condition, we also monitored the effect of incubation time on the currents of the assay system (*Note*: To avoid confusion, the incubation times of the Ω DNA nanostructures with target ATP were paralleled with those of ATP-S_A with hemin). As shown in Fig. 2b, the SWV peak currents increased with the increment of incubation time, and tended to level off after 10 min. Longer incubation times did not almost cause the significant increase in the detectable signal. Thus, pH 6.8 BR buffer and an incubation time of 10 min were selected for sensitive determination of target ATP at acceptable throughout.

Under the optimal conditions, the sensitivity and quantitative range of the developed homogeneous assay were evaluated by using the as-prepared Ω DNA nanostructures as the recognition elements. The measurement was carried out in pH 6.8 BR buffer containing 10 μM hemin, 0.02 M OPD and 0.02% (v/v) H_2O_2. As shown from the inset of Fig. 3a, the currents increased with the increasing ATP concentrations from 0 to 10 nM in the sample. Two linear relationships between the peak currents and the ATP standards were obtained within the range of 1.0 pM - 10 nM (*i.e.*, 1.0 pM - 0.1 nM and 0.1 nM - 10 nM). The linear regression equations were i (μA) = 29.718 × $C_{[ATP]}$ + 6.6683 (nM, R^2 = 9943, n = 21) for 1.0 pM - 0.1 nM and i (μA) = 0.4496 × $C_{[ATP]}$ + 10.022 (nM, R^2 = 0.9952, n = 18) for 0.1 nM - 10 nM, respectively. The detection limit was 0.6 pM estimated at the 3δ criterion. The reason might be the fact that the binding reaction between ATP and the aptamer was more easily carried out when the amount of the Ω DNA nanostructures was excessively higher than that of target analyte, thus resulting in the strong change in the signal within the low-concentration range.

To monitor the precision and reproducibility of determinations, we repeatedly assayed 3 different-concentration ATP standards, using identical batches of Ω DNA nanostructures. Experimental results indicated that the coefficients of variation (CVs) of the intra-assay between five runs were 7.5%, 9.1%, and 8.3% for 1 pM, 0.1 nM, and 1 nM ATP, respectively, whereas the CVs of the inter-assay with various batches were 10.2%, 9.3%, and 9.8% towards the above mentioned analyte. Hence, both intra-assay and interassay verified acceptable reproducibility and further revealed the possibility of batch preparation.

The specificity and sample matrix effect were also investigated by challenging the system with 3 ATP analogues (*i.e.*, cytidine triphosphate: CTP; guanosine triphosphate: GTP; and uridine triphosphate: UTP) and other proteins (*e.g.*, human IgG; human serum albumin, BSA; human serum albumin, HSA). The assay was implemented with the same experimental procedures. As shown from Fig. 3b, a significant change in the current was observed with Target ATP toward 10-fold higher interfering components. Thus, the developed homogeneous assay was shown to be sufficiently selective for the detection of ATP.

To further monitor the possible application of the developed strategy for analysis of real samples, 4 ATP standards including 1.0 pM, 10 pM, 0.1 nM and 1.0 nM ATP were spiked into blank new-born calf serum, respectively. Then, these samples were measured by using the homogeneous assay protocol, respectively. The assayed results were calculated according to the mentioned-above linear regression equation. Experimental results displayed that ATP levels in the four serum samples were 0.81 ± 0.7 pM, 10.19 ± 0.12 pM, 0.14 ± 0.05 nM and 1.21 ± 1.3 nM ATP, respectively (n = 3). The recoveries were 81 – 140%. Therefore, the methodology could be utilized for the detection of target ATP in real samples.

In summary, we successfully constructed a new homogeneous electrochemical assay system for sensitive detection of ATP (as a model) by coupling with an omega-like DNA nanostructure. The signal was amplified through target-stimulated conformational change of DNA nanostructures accompanying the formation of DNAzyme. Compared with conventional aptamer-based electrochemical assay methods, the designed Ω DNA nanostructures are simple, feasible and label-free. Importantly, the assay procedure can avoid the sample separation and multi-step washing. Thus,

the homogeneous electrochemical assay can potentially benefit on-site monitoring applications.

Support by the "973" National Basic Research Program of China (2010CB732403), the NSFC of China (21075019 & 41176079), the Research Fund for the Doctoral Program of Higher Education (20103514120003), the NSF of Fujian Province (2011J06003), and Program for Changjiang Scholars and Innovative Research Team in University (IRT1116) is gratefully acknowledged.

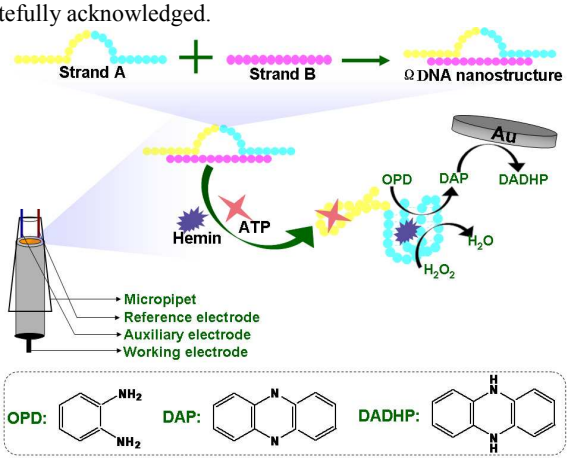

Scheme 1 Schematic illustration of the homogeneous electronic monitoring system toward target ATP by using target-triggered formation of DNAzyme-aptamer conjugate on an omega-like DNA nanostructure.

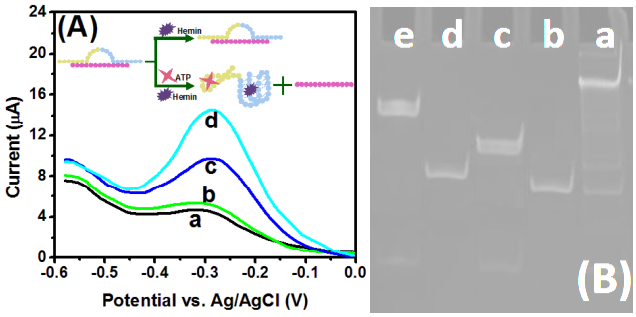

Fig. 1 (A) SWV curves of (a) Ω DNA nanostructures, (b) probe '*a*' + 10 μM hemin, (c) probe '*b*' + 0.1 nM ATP, and (d) probe '*b*' + 10 nM ATP in pH 6.8 BR buffer containing 0.02 M OPD and 0.02% H_2O_2. (B) Gel electrophoresis (lane a: DNA marker, lane b: Ω DNA nanostructures, lane c: Ω DNA + 10 nM ATP, lane d: Ω DNA + 10 μM hemin, lane e: Ω DNA + 10 nM ATP + 10 μM hemin).

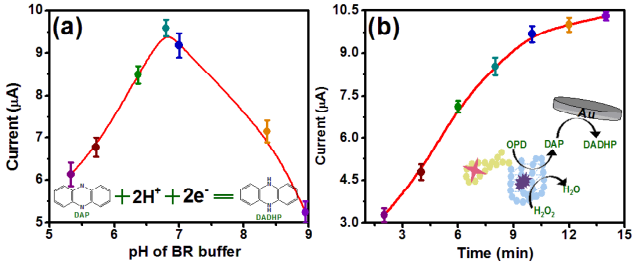

Fig. 2 The effect of (b) pH of BR buffer and (b) incubation time on the electrochemical signal of the homogenous assay system (0.1 nM ATP used in this case).

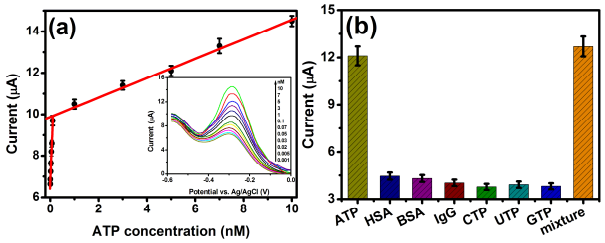

Fig. 3 (a) Calibration plots of the electrochemical assay system toward ATP standards with various concentrations (*Inset*: The corresponding SWV curves in pH 6.8 BR buffer containing 0.02 M OPD and 0.02% H_2O_2). (b) The specificity of the developed method against HSA, BSA, IgG, ATP, CTP, UTP, GTP, and mixture (containing ATP, HBA, BSA, IgG, CTP, UTP and GTP).

Notes and references

Ministry of Education Key Laboratory of Analysis and Detection of Food Safety, Fujian Provincial Key Laboratory of Analysis and Detection of Food Safety, Department of Chemistry and Chemical Engineering, Fuzhou University, Fuzhou 350108, P.R. China. Fax: +86 591 22866135; E-mail: dianping.tang@fzu.edu.cn (D. Tang)

† Electronic supplementary information (ESI) available: experimental section. See DOI: 10.1039/xxxxxxx

1 (*a*) F. Rohrbach, F. Schafer, M. Fichte, F. Pfeiffer, J. Muller, B. Potzsch, A. Heckel and G. Mayer, *Angew. Chem. Int. Ed.,* 2013, **52**, 11912; (b) X. Zhang, M. Bttig and Y. Wang, *Chem. Commun*., 2013, **49**, 9600.

2 (*a*) K. Li, W. Qin, F. Li, X. Zhao, B. Jiang, K. Wang, S. Deng, C. Fan and D. Li, *Angew. Chem. Int. Ed*., 2013, **52**, 11542; (*b*) A. Kent, N. Spiropulos and J. Heemstra, *Anal. Chem*., 2013, **85**, 9916; (*c*) Q. Zhao and J. Gao, *Chem. Commun*., 2013, **49**, 7720; (*d*) D. Tang, J. Tang, Q. Li, B. Su and G. Chen, *Anal. Chem*., 2011, **83**, 7255.

3 (*a*) C. Li, Z. Wang, T. Gao, A. Duan and G. Li, *Chem. Commun*., 2013, **49**, 3760; (*b*) S. Liu, Y. Wang, C. Zhang, Y. Lin and F. Li, *Chem. Commun*., 2013, **49**, 2335; (*c*) K. Karns, J. Vogan, Q. Qin, S. Hichey, S. Wilson, M. Hammond and A. Herr, *J. Am. Chem. Soc*., 2013, **135**, 3136.

4 (*a*) J. Liu, C. Wang, Y. Jiang, Y. Hu, J. Li, S. Yang, Y. Li, R. Yang, W. Tan and C. Huang, *Anal. Chem*., 2013, **85**, 1424; (*b*) Q. Xu, A. Cao, L. Zhang and C. Zhang, *Anal. Chem*., 2012, **84**, 10845.

5 (*a*) J. Zhuang, L. Fu, W. Lai, D. Tang, G. Chen, Chem. Commun., 2013, **49**, 11200; (*b*) J. Tang, J. Zhou, Q. Li, D. Tang, G. Chen, H. Yang, *Chem. Commun*., 2013, **49**, 1530; (*c*) B. Zhang, B. Liu, D. Tang, R. Niessner, G. Chen and D. Knopp, *Anal. Chem*., 2012, **84**, 5392.

6 (*a*) N. Kaneko, K. Horii, S. Kato, J. Akitomi and I. Waga, *Anal. Chem*., 2013, **85**, 5430; (*b*) M. Xu, J. Zhuang, X. Chen, G. Chen, D. Tang, *Chem. Commun*., 2013, **49**, 7304; (*c*) J. Tang, L. Hou, D. Tang, B. Zhang, J. Zhu and G. Chen, *Chem. Commun*., 2012, **48**, 8180.

7 (*a*) C. Wang, G. Jia, Y. Li, S. Zhang and C. Li, *Chem. Commun*., 2013, **49**, 11161; (*b*) P. Murat, M. Gormaly, D. Sanders, M. Antonio and S. Balasubramanian, *Chem. Commun*., 2013, **49**, 8453; (*c*) H. Zhou, Y. Zhang, J. Liu, J. Xu and H. Chen, *Chem. Commun*., 2013, **49**, 2246.

8 (*a*) R. Haudecoeur, L Stefan, F. Denat and D. Monchaud, *J. Am. Chem. Soc*., 2013, **135**, 550; (*b*) X. Wang, Z. Ding, Q. Ren and W. Qin, *Anal. Chem*., 2013, **85**, 1945; (*c*) V. Pradines and G. Pratviel, *Angew. Chem. Int. Ed*., 2013, **52**, 2185.

9 (*a*) O. Wilner and I. Willner, *Chem. Rev*., 2012, **112**, 2528; (*b*) X. Liu, R. Aizen, R. Freeman, O. Yehezkeli and I. Willner, *ACS Nano*, 2012, **6**, 3553; (*c*) Z. Zhang, D. Balogh, F. Wang and I. Willner, *J. Am. Chem. Soc.*, 2013, **135**, 1934.

10 (*a*) C. Fu, X. Zheng, Y. Jiang, Y. Liu, P. Xu, Z. Zeng, R. Liu and Y. Zhao, *Chem. Commun*., 2013, **49**, 2795; (*b*) Q. Xue, L. Wang and W. Jiang, *Chem. Commun*., 2013, *49*, 2640.